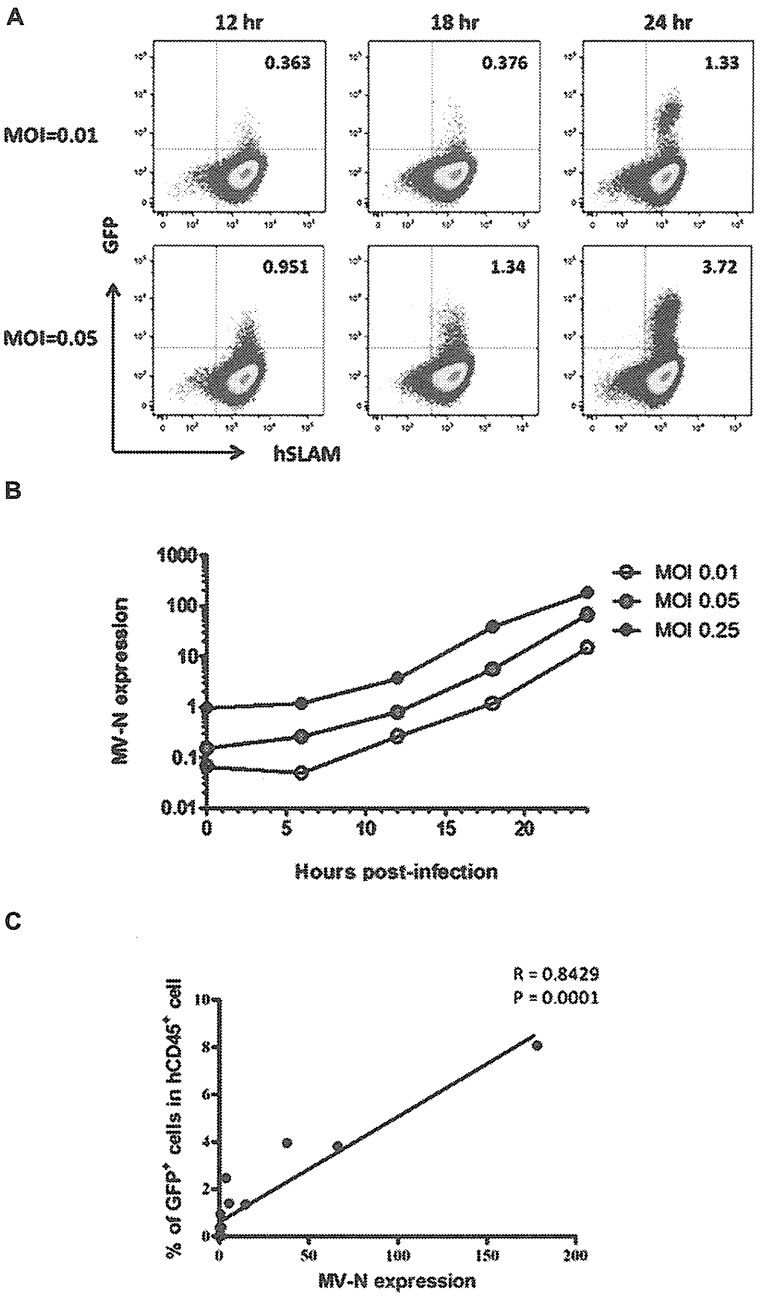

FIGURE 2 | Time course of MV infection *in vitro*. Jurkat/hSLAM cells were infected with wild-type MV IC323-EGFP at MOI of 0.01, 0.05, and 0.25, washed, and harvested at the indicated time points. **(A)** Cells were stained with PE-conjugated anti-hSLAM mAb, fixed with 2% formalin/PBS, and GFP expression was analyzed. **(B)** RNA was extracted from cells, and expression levels of MV-N and RNase P were analyzed by one-step qRT-PCR. The copy numbers of MV-N and RNase P were determined, and the ratio of MV-N copies to RNase P copies is depicted on the vertical axis. **(C)** Correlation between the percentage of GFP^+ Jurkat/SLAM cells and the time course of MV-N expression. Spearman's rank correlation coefficient was used for statistical analysis.

cell frequencies by flow cytometry. Next, we extracted RNA from PBMCs and BM cells and analyzed MV-N expression by qRT-PCR, as described in the previous section. MV-N expression paralleled the GFP^+ frequencies in BM (**Figure 3B**). Notably, a high level of MV-N expression was also detected in PBMCs of mouse 127-4, suggesting that the level of MV-N expression per single hematopoietic cell is similar between blood and BM. We plotted the GFP^+ frequency and MV-N expression level in BM cells of eight mice. As shown in **Figure 3C**, these values were well correlated ($R = 0.9286$). Taken together, these data indicate that MV infection *in vivo* is detectable in BM by both flow cytometry and MV-N RNA qRT-PCR analysis, but only MV-N RNA qRT-PCR is

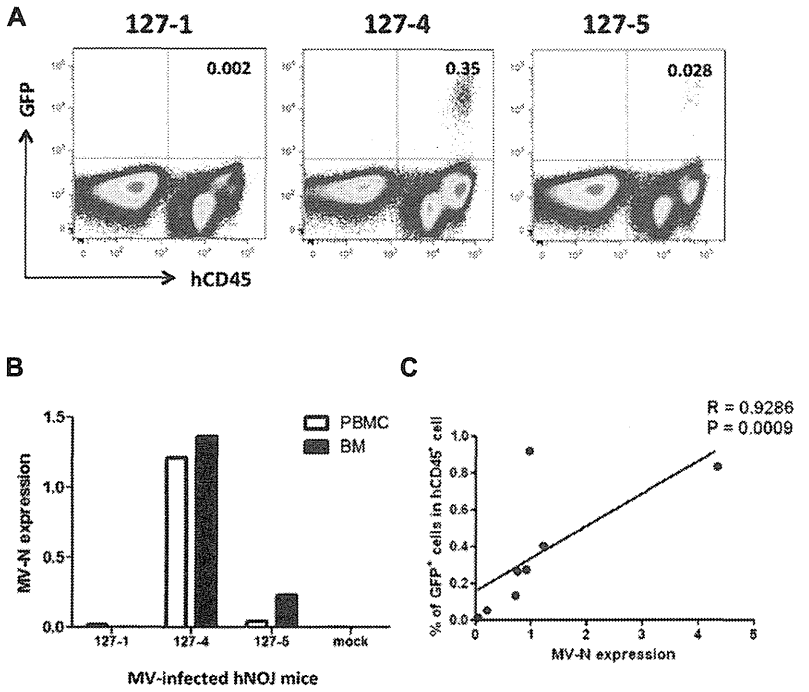

FIGURE 3 | Analysis of MV infection *in vivo*. Three hNOJ mice (127-1, -4, and -5) were infected intravenously with 2,000 pfu of the MV vaccine strain, AIK-C-EGFP. Mice were sacrificed at day 7 post-infection, and blood and bone marrow cells (BM) were obtained. **(A)** BM cells were stained with PB-anti-human CD45 mAb, fixed with 2% formalin/PBS, and GFP expression was analyzed. **(B)** PBMCs from blood and BM cells were lysed, and RNA was prepared. The expression MV-N and RNase P was analyzed as described in the legend for **Figure 2B**. **(C)** Correlation between the percentage of GFP^+ cells among $hCD45^+$ cells in BM and the level of MV-N expression in MV-infected hNOJ mice, at day 7 ($n = 4$) or day 10 ($n = 4$) p.i. Spearman's rank correlation coefficient was used for statistical analysis.

sensitive enough to detect PBMC-associated MV infection in the blood.

KINETICS OF MV GROWTH CAN BE MONITORED IN THE BLOOD OF hNOJ MOUSE

Finally, we measured MV growth kinetics *in vivo* by qRT-PCR analysis using sequential blood samples obtained from MV-infected hNOJ mice; it was not feasible to perform these measurements by flow cytometry because of the paucity of human PBMCs in the blood. Two or three hNOJ mice in each group were infected intravenously with 200, 2000, or 20,000 pfu AIK-C-EGFP and followed up to 21 days p.i. The level of PBMC-associated MV RNA in individual mice is shown in **Figure 4A**. We noticed two peaks of MV replication, the first at around day 3 p.i., and the second at day 10 p.i., irrespective of the initial inoculum. Two mice infected with 20,000 pfu MV exhibited a high level of MV replication that peaked at day 10 p.i. One mouse infected with 2,000 pfu exhibited a high level of MV replication at day 3 p.i., followed by a small peak at day 10 p.i. For some mice, we counted the number of human cells per 50 μl of blood used for RNA extraction. The data are shown in **Figure 4B**. We were able to detect high levels of MV in samples containing less than 2,000 cells, indicating that the qRT-PCR system is sensitive enough to detect low numbers of MV-infected human cells.

Although MV replication was not obvious in three mice infected with the smallest dose (200 pfu), one of these animals exhibited an increase in MV RNA expression at day 21 p.i. (gray circle). We sacrificed this particular mouse and used flow cytometry to analyze GFP expression in its blood, spleen, MLN, and BM. As shown in **Figure 4C**, GFP^+ cells were present in spleen (0.308%) and all the other tissues, albeit at a lower frequency, indicating that MV infection can occur even at a low dose (200 pfu) and spread slowly in the systemic lymphoid tissues of hNOJ.

It may be necessary to acquire at least 30,000 events to be sure of having >10,000 cells for flow cytometry analysis. This is because of the substantial amount of sample loss that occurs in this system. The flow cytometry data presented in **Figure 4C** were obtained by analyzing ~0.4 ml blood from a sacrificed mouse. However, even under these conditions, the proportion of MV-infected cells detected was only 0.056%; indeed, the cells are barely visible on the plot. Therefore, it appears that flow cytometry is not a suitable method for the sequential monitoring of infected (GFP^+) cells. Thus, the qRT-PCR system we have developed here allowed us to monitor systemic MV replication using a small volume of blood from humanized mice.

DISCUSSION

Based on a highly sensitive MV-N RNA detection method previously developed by Hummel et al. (2006), which could detect one copy of synthetic MV RNA/reaction, we developed a novel one-step real-time qRT-PCR system for the purpose of monitoring MV replication in the blood of MV-infected humanized mice.

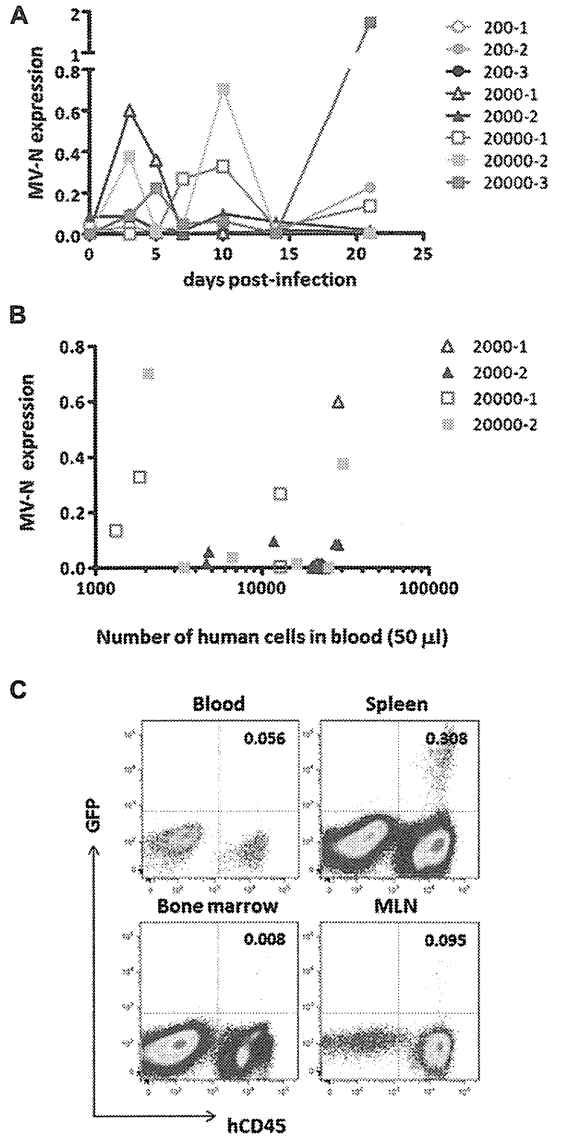

FIGURE 4 | Monitoring of MV replication *in vivo*. Two to three hNOJ mice per group were challenged with MV AIK-C-EGFP at 20,000 (squares), 2,000 (triangles), or 200 pfu (circles). The PBMCs of these mice were collected at day 3, 5, 7, 10, 14, and 21 p.i. **(A)** The level of MV-N expression in the blood of infected hNOJ. Vertical axis shows the level of MV-N relative to that of RNaseP, as described in the legend for **Figure 2B**.**(B)** For some mice (depicted using the same symbol as **(A)**), the number of human cells per 50 μl of blood used for RNA extraction and analyzed for MV-N expression was plotted on the X-axis. **(C)** An hNOJ mouse infected with MV at a low dose (gray closed circle, 200-2) exhibited an increased level of MV-N. At day 21 p.i., the mouse was sacrificed; cells from blood, spleen, BM, and mesenteric lymph node (MLN) were prepared. Cells were stained and analyzed as described in the legend for **Figure 2A**.

Because MV replication usually occurs in association with cells (Griffin, 2007), it is necessary to evaluate the endogenous RNA expression level of human PBMCs that co-exist with mouse blood cells. To this end, we designed human-specific primer/probe sets for the CD45 and RNase P mRNAs. When we analyzed the detection efficiencies of these two primer/probe sets using distinct cell types present in human PBMCs, we found that RNase P expression was less dependent than CD45 expression on cell type. Using this qRT-PCR system with RNase P as an internal control, we can reliably detect MV replication with high sensitivity in humanized mice *in vivo*. When MV expressing GFP was used for infections *in vitro* or *in vivo*, the level of MV-N RNA was closely correlated with the frequencies of GFP^+ MV-infected cells determined by flow cytometry.

Our qRT-PCR system allowed us to follow MV replication *in vivo* using a small amount of blood, with no need to sacrifice mice at each time point. Although flow-cytometric analysis provides valuable information, such as the proportions of various cell types and the surface phenotypes of MV-infected cells, the small number of human cells circulating in the mouse blood may not be sufficient for precise estimation of MV-infected cells by flow cytometry. By contrast, our qRT-PCR system was able to detect MV-N RNA in fewer than 2,000 human PBMCs (**Figure 4B**). This is an important technological advantage considering that individual humanized mice exhibit variable levels of human cell engraftment, i.e., chimerism (Terahara et al., 2013); moreover, there may exist donor-to-donor variation in susceptibility to MV infection. Thus, it should be possible to select humanized mice with a degree of MV infection appropriate for the purpose of a given experiment.

In this study, MV was inoculated through the tail vein, and infected cells were distributed to systemic lymphoid tissues as well as BMs, where human hematopoietic cells localize in humanized mice (Traggiai et al., 2004). MV may also be distributed to other organs, such as lung and intestinal tissue, as demonstrated in the case of HIV infection using the BLT mouse (Sun et al., 2007). To our surprise, by monitoring MV replication in PBMCs of humanized mice, we noticed two peaks of MV replication, at around 3 and 10 days p.i., in some mice. This pattern of MV replication did not depend on the initial dose of MV inoculum. We do not know why MV replication showed two peaks in many animals. However, it was recently reported in a monkey model that MV RNA persists in PBMCs for more than 1 month after primary infection, and declined in three phases (Lin et al., 2012). The authors of that study hypothesized that both T cells, including regulatory T cells (Treg), and antibody responses contributed to the dynamics of MV replication *in vivo*. Although hNOJ mice are reported to show poor immune responses, the role of regulatory T cells should be considered. This is because these cells regulate HIV-1 infection in humanized mice (Jiang et al., 2008). Alternatively, it may be that the intravenous injection of MV rapidly kills the target cells (probably those showing an activated phenotype) within 3 days. The low number of MV-infected cells then gradually transmits the virus to the human cells that are replenished from the BM stem cell pool. Further investigations are required to clarify this issue.

The humanized mouse model is expected to be a useful tool for studying virus infection (Akkina, 2013). Although the human immune system is not fully reconstructed by the transplantation of human HSCs alone, we believe that further improvements are possible, which will allow us to utilize this mouse model to not only evaluate vaccine and drug efficacy but also to increase our understanding of the pathogenesis of MV infection. The described novel method of monitoring MV-infected human cells in the blood will

be useful for studying MV-based vaccines in humanized mouse models without the need to sacrifice the mice.

ACKNOWLEDGMENTS

We thank Prof. Yusuke Yanagi for providing IC323-EGFP, and Ms. Kahori Okano for her excellent technical assistance. We also thank the Tokyo Cord Blood Bank for donating human umbilical cord blood. This work was supported in part by a grant from the Ministry of Health, Labor, and Welfare of Japan, and in part by a grant from the Ministry of Education, Science, Sports, and Culture of Japan. Shota Ikeno is supported by the Global COE Program (Practical Chemical Wisdom) from the Ministry of Education, Culture, Sports, Science, and Technology of Japan.

REFERENCES

Akkina, R. (2013). New generation humanized mice for virus research: comparative aspects and future prospects. *Virology* 435, 14–28. doi: 10.1016/j.virol.2012.10.007

Brandler, S., Marianneau, P., Loth, P., Lacote, S., Combredet, C., Frenkiel, M. P., et al. (2012). Measles vaccine expressing the secreted form of West Nile virus envelope glycoprotein induces protective immunity in squirrel monkeys, a new model of West Nile virus infection. *J. Infect. Dis.* 206, 212–219. doi: 10.1093/infdis/jis328

Despres, P., Combredet, C., Frenkiel, M. P., Lorin, C., Brahic, M., and Tangy, F. (2005). Live measles vaccine expressing the secreted form of the West Nile virus envelope glycoprotein protects against West Nile virus encephalitis. *J. Infect. Dis.* 191, 207–214. doi: 10.1086/426824

Fujino, M., Yoshida, N., Kimura, K., Zhou, J., Motegi, Y., Komase, K., et al. (2007). Development of a new neutralization test for measles virus. *J. Virol. Methods* 142, 15–20. doi: 10.1016/j.jviromet.2007.01.001

Griffin, D. E. (2007). "Measles virus," in *Fields Virology*, eds D. M. Knipe, P. M. Howley, D. E. Griffin, R. A. Lamb, M. A. Martin, B. Roizman, and S. E. Straus, 5 Edn (Philadelphia: Lippincott Williams & Wilkins, a Wolters Kluwer Business), 1551–1585.

Hamaia, S., Li, C., and Allain, J. P. (2001). The dynamics of hepatitis C virus binding to platelets and 2 mononuclear cell lines. *Blood* 98, 2293–2300. doi: 10.1182/blood.V98.8.2293

Hashimoto, K., Ono, N., Tatsuo, H., Minagawa, H., Takeda, M., Takeuchi, K., et al. (2002). SLAM (CD150)-independent measles virus entry as revealed by recombinant virus expressing green fluorescent protein. *J. Virol.* 76, 6743–6749. doi: 10.1128/JVI.76.13.6743-6749.2002

Hummel, K. B., Lowe, L., Bellini, W. J., and Rota, P. A. (2006). Development of quantitative gene-specific real-time RT-PCR assays for the detection of measles virus in clinical specimens. *J. Virol. Methods* 132, 166–173. doi: 10.1016/j.jviromet.2005.10.006

Ito, R., Takahashi, T., Katano, I., and Ito, M. (2012). Current advances in humanized mouse models. *Cell. Mol. Immunol.* 9, 208–214. doi: 10.1038/cmi.2012.2

Jiang, Q., Zhang, L., Wang, R., Jeffrey, J., Washburn, M. L., Brouwer, D., et al. (2008). FoxP3+CD4+ regulatory T cells play an important role in acute HIV-1 infection in humanized Rag2−/−gammaC−/− mice in vivo. *Blood* 112, 2858–2868. doi: 10.1182/blood-2008-03-145946

Kato, S. I., Nagata, K., and Takeuchi, K. (2012). Cell tropism and pathogenesis of measles virus in monkeys. *Front. Microbiol.* 3:14. doi: 10.3389/fmicb.2012.00014

Kimberly, W. T., Zheng, J. B., Town, T., Flavell, R. A., and Selkoe, D. J. (2005). Physiological regulation of the beta-amyloid precursor protein signaling domain by c-Jun N-terminal kinase JNK3 during neuronal differentiation. *J. Neurosci.* 25, 5533–5543. doi: 10.1523/JNEUROSCI.4883-04.2005

Koga, R., Ohno, S., Ikegame, S., and Yanagi, Y. (2010). Measles virus-induced immunosuppression in SLAM knock-in mice. *J. Virol.* 84, 5360–5367. doi: 10.1128/JVI.02525-09

Lin, W. H., Kouyos, R. D., Adams, R. J., Grenfell, B. T., and Griffin, D. E. (2012). Prolonged persistence of measles virus RNA is characteristic of primary infection dynamics. *Proc. Natl. Acad. Sci. U.S.A.* 109, 14989–14994. doi: 10.1073/pnas.1211138109

Lorin, C., Mollet, L., Delebecque, F., Combredet, C., Hurtrel, B., Charneau, P., et al. (2004). A single injection of recombinant measles virus vaccines expressing human immunodeficiency virus (HIV) type 1 clade B envelope glycoproteins induces neutralizing antibodies and cellular immune responses to HIV. *J. Virol.* 78, 146–157. doi: 10.1128/JVI.78.1.146-157.2004

Ohno, S., Ono, N., Seki, F., Takeda, M., Kura, S., Tsuzuki, T., et al. (2007). Measles virus infection of SLAM (CD150) knockin mice reproduces tropism and immunosuppression in human infection. *J. Virol.* 81, 1650–1659. doi: 10.1128/JVI.02134-06

Reyes-del Valle, J., Hodge, G., Mcchesney, M. B., and Cattaneo, R. (2009). Protective anti-hepatitis B virus responses in rhesus monkeys primed with a vectored measles virus and boosted with a single dose of hepatitis B surface antigen. *J. Virol.* 83, 9013–9017. doi: 10.1128/JVI.00906-09

Sawada, A., Komase, K., and Nakayama, T. (2011). AIK-C measles vaccine expressing fusion protein of respiratory syncytial virus induces protective antibodies in cotton rats. *Vaccine* 29, 1481–1490. doi: 10.1016/j.vaccine.2010.12.028

Sellin, C. I., and Horvat, B. (2009). Current animal models: transgenic animal models for the study of measles pathogenesis. *Curr. Top. Microbiol. Immunol.* 330, 111–127. doi: 10.1007/978-3-540-70617-5_6

Singh, M., Cattaneo, R., and Billeter, M. A. (1999). A recombinant measles virus expressing hepatitis B virus surface antigen induces humoral immune responses in genetically modified mice. *J. Virol.* 73, 4823–4828.

Stebbings, R., Fevrier, M., Li, B., Lorin, C., Koutsoukos, M., Mee, E., et al. (2012). Immunogenicity of a recombinant measles-HIV-1 clade B candidate vaccine. *PLoS ONE* 7:e50397. doi: 10.1371/journal.pone.0050397

Sun, Z., Denton, P. W., Estes, J. D., Othieno, F. A., Wei, B. L., Wege, A. K., et al. (2007). Intrarectal transmission, systemic infection, and CD4+ T cell depletion in humanized mice infected with HIV-1. *J. Exp. Med.* 204, 705–714. doi: 10.1084/jem.20062411

Tatsuo, H., Ono, N., Tanaka, K., and Yanagi, Y. (2000). SLAM (CDw150) is a cellular receptor for measles virus. *Nature* 406, 893–897. doi: 10.1038/35022579

Terahara, K., Ishige, M., Ikeno, S., Mitsuki, Y. Y., Okada, S., Kobayashi, K., et al. (2013). Expansion of activated memory $CD4^+$ T cells affects infectivity of CCR5-tropic HIV-1 in humanized NOD/SCID/JAK3^{null} mice. *PLoS ONE* 8:e53495. doi: 10.1371/journal.pone.0053495

Traggiai, E., Chicha, L., Mazzucchelli, L., Bronz, L., Piffaretti, J. C., Lanzavecchia, A., et al. (2004). Development of a human adaptive immune system in cord blood cell-transplanted mice. *Science* 304, 104–107. doi: 10.1126/science.1093933

Wege, A. K., Melkus, M. W., Denton, P. W., Estes, J. D., and Garcia, J. V. (2008). Functional and phenotypic characterization of the humanized BLT mouse model. *Curr. Top. Microbiol. Immunol.* 324, 149–165. doi: 10.1007/978-3-540-75647-7_10

Conflict of Interest Statement: The authors declare that the research was conducted in the absence of any commercial or financial relationships that could be construed as a potential conflict of interest.

Received: 07 August 2013; accepted: 17 September 2013; published online: 11 October 2013.

Citation: Ikeno S, Suzuki M, Muhsen M, Ishige M, Kobayashi-Ishihara M, Ohno S, Takeda M, Nakayama T, Morikawa Y, Terahara K, Okada S, Takeyama H and Tsunetsugu-Yokota Y (2013) Sensitive detection of measles virus infection in the blood and tissues of humanized mouse by one-step quantitative RT-PCR. Front. Microbiol. 4:298. doi: 10.3389/fmicb.2013.00298

This article was submitted to Virology, a section of the journal Frontiers in Microbiology.